Transmission Estimation in Underwater Single Images

P. Drews-Jr[1,2], E. do Nascimento[2], F. Moraes[1], S. Botelho[1], M. Campos[2]
[1]C3 - Univ. Federal do Rio Grande (FURG)
Rio Grande - Brazil
{paulodrews,fmoraes,silviacb}@furg.br
[2]DCC - Univ. Federal de Minas Gerais (UFMG)
Belo Horizonte - Brazil
{erickson,mario}@dcc.ufmg.br

Abstract

This paper proposes a methodology to estimate the transmission in underwater environments which consists on an adaptation of the Dark Channel Prior (DCP), a statistical prior based on properties of images obtained in outdoor natural scenes. Our methodology, called Underwater DCP (UDCP), basically considers that the blue and green color channels are the underwater visual information source, which enables a significant improvement over existing methods based in DCP. This is shown through a comparative study with state of the art techniques, we present a detailed analysis of our technique which shows its applicability and limitations in images acquired from real and simulated scenes.

1. Introduction

In images acquired in a participating medium, the light suffers absorption and scattering by the medium before reaches the camera. It generated an effect called *haze*. Basically, haze becomes a serious issue since it reduces the overall contrast in images and causes color shift, directly impacting on the reduction in the visibility. Therefore, dehazing an image plays a fundamental role in the restoration process of an image that will be further processed by legacy computer vision algorithms. The main challenge in the dehazing process, as well as with many other underwater restoration methods, is obtaining the true scene appearance, *i.e.*, the appearance that the scene would have if it were not immersed in that specific medium.

More specifically, the problem of restoring underwater images has been approach from several angles in the literature: using specialized hardware [8], multiple images under different conditions [15], stereo images [17, 16] and polarization filters [19]. Despite the good results, the methods that rely on specialized hardware are expensive and complex. Furthermore, they are hard to implement when more automatic acquisition is required. In the stereo systems approach, the correspondence problem becomes even harder due to the strong effects imposed by the participating medium. Methods based on multiple images require several images of the same scene taken in different environment conditions, which makes it of difficult application in real conditions. Therefore, in spite of the advances that have already been reached, the problem of image restoration for underwater scenes still demands much research effort.

Recently, several dehazing algorithms using a single image have been proposed [6, 20, 9]. While dehazing methods have shown good performance for outdoor terrestrial images, there is still room for improvement when they are applied to underwater images. One key aspect that needs to be probed further is the transmission estimation, which is based on heuristics, which may hold true only for restricted conditions.

As far as single image methods are concerned, He *et al.* [9, 11] proposed a new methodology called Dark Channel Prior (DCP). Their approach is based on the observations that haze-free images have at least one color in the RGB spectrum with low intensity value. More recently, the DCP methodology has also been applied in underwater image restoration [3, 4]. However, those works do not address some of the key DCP limitations and the required changes in the assumptions. Thus, the main contribution of the present work is the adaptation of the DCP in order to overcome its limitations for applications in underwater imaging.

2. Methodology

2.1. Optical Model

The images captured in a participating medium can be modeled as a complex interaction between the light, the medium and the scene. The model proposed by Jaffe-McGlamery [13, 12] is one of the most used in the literature. This model is composed of three components: direct illumination (E_d), forward-scattering (E_{fs}) and backscattering (E_{bs}), as shown in Eq. 1:

$$E_T = E_d + E_{fs} + E_{bs}. \quad (1)$$

The direct component is the fraction of light that reaches the camera. Part of the light that irradiates from object is

lost due to scattering and absorption. This effect should be considered in the direct component. According to Schechner and Karpel [19], backscattering is the prime reason for image contrast degradation, thus the forward-scattering can be neglected. Indeed, this assumption is valid, since the average depth between the scene and the camera is large. After simplifications and following the nomenclature used in [9, 11], the direct component is defined as:

$$E_d = Je^{-\eta d} = Jt, \tag{2}$$

where J and d are the scene radiance and depth, respectively, and η is the attenuation coefficient (also termed c in the literature), and t is the medium transmission, considered as the exponential term.

In outdoor scenes, the attenuation coefficient η is composed only of the scattering coefficient, called β in [9]. In underwater environments, the absorption represents the inherent properties of the medium [12], thus the coefficient η is the sum of the absorption coefficient, a, and scattering, β; where both are wavelength dependent.

The backscattering component does not originate from the object's radiance, but it results from the interaction between the ambient illumination sources and particles dispersed in the medium. Therefore, a simplified model can be written as:

$$E_{bs} = A(1 - e^{-\eta d}) = A(1 - t), \tag{3}$$

where the A is the airlight or the global light in the scene, also called B_∞ in the literature. It is a scalar that depends on the wavelength. The other terms are the same as for the direct components.

Therefore, an enhanced model that describes the formation of an image in participating medium can be stated as:

$$I(x) = J(x)t(x) + A(1 - t(x)), \tag{4}$$

where x are the pixel coordinates and I is the image obtained in a participating medium. This model is valid assuming that the medium is homogeneous.

2.2. Dark Channel Prior (DCP)

The Dark Channel Prior is a statistical prior based on the observation that clear day images exhibited a mostly dark image in a square patch of the image. It was firstly proposed in [9], and extended in [11]. The authors consider that in most of the nonsky patches, at least one color channel has some pixels whose intensity are almost zero. These low intensity in the dark channel is due to three factors, as described in [9, 11]: a) shadows in the images; b) colorful objects or surfaces where at least one color has low intensity and c) dark objects or surfaces. They collected a large number of outdoor images and build histograms, and with that, they have shown that about 75 percent of the pixels in the dark channel have zero values, and the intensity of 90 percent of the pixels is below 25. Those results provide a strong support to the dark channel prior assumption for outdoor images.

The formal description of the DCP prior defines the concept of dark channel as:

$$J^{dark}(x) = \min_{y \in \Omega(x)} (\min_{c \in R,G,B} J^c(y)), \tag{5}$$

where J^c is a scene radiance for each color channel and $\Omega(x)$ is a local patch centered at x. Using this model, the observation allow us to say that if J is a haze-free image, except for the sky region, the intensity of J is low and tends to zero ($J^{dark} \to 0$).

Considering the optical model it is possible to estimate the transmission based on the DCP. The airlight constant A can be estimated in different ways: Using calibration [7], finding the farthest pixel in the scene [16, 17], finding the brightest pixel in the image [20, 6] or finding the brightest pixel in the dark channel [9, 11]. Considering Eqs. 4 and 5, it is possible to isolate the transmission in a local patch $\tilde{t}$ using DCP. Applying the minimum operation to both sides of the equation, we can estimate $\tilde{t}$ based on the image I and the airlight A. Eq. 6 shows the estimation of $\tilde{t}$.

$$\tilde{t}(x) = 1 - \min_{y \in \Omega(x)} (\min_{c \in R,G,B} \frac{I^c(y)}{A^c}). \tag{6}$$

The transmission $\tilde{t}$ is only one approximation of the transmission due simplifications.The use of a local patch affects the performance of the transmission estimation. He *et al.* [9] proposed the use of a spectral matting method to refine the estimated transmission. Their method works well but requires a high computational power to process the Laplacian matrix. This method can be approximated, as described in [10], in order to make it faster. The use of quadtrees was also proposed as a way to reduce the computation when solving the problem [5]. Other possibility to refine the transmission is using Markov Random Fields, as proposed in [6, 20].

2.3. DCP in Underwater Condition

Due to the good results obtained by the work of He *et al.* [9, 11] and the similarities in the optical model of a haze image and an underwater image, some works using DCP to restore underwater image were proposed in the literature. One of the first works to use DCP was [3], where the methodology proposed by He *et al.* [9, 11] was directly applied in underwater images. The results show a limited number of experiments where the visual quality of the result does not show significant improvement, even in images with small degradation. However, the authors raise an important issue related to the normalized image (I^c/A), that it reduces the

effect of color absorption for different wavelength in underwater images.

Similarly, Chiang *et al.* [4] proposed an underwater image restoration method using standard DCP in order to find the transmission map t. They consider that the attenuation coefficient η is known *a priori*. This allows finding the depth map, instead of the transmission. Furthermore, they also proposed a method to estimate the water depth where the image was acquired. Their method obtains good results for real underwater images, but it is limited by the standard DCP method in underwater images and by the assumption that the image is predominantly blue.

Bianco *et al.* [2] proposed a underwater single image dehazing using a new interpretation of the DCP for underwater conditions. The prior proposed explores the fact that the attention of light in water varies depending of the color of the light, *i. e.*, the wavelength. In underwater medium, the red color channel is attenuated at a much higher rate than the green or blue. The prior is shown in the Eq. 7, and called BP in this work. Differently from the standard DCP, this prior is based on the difference between the maximum in the red channel and the other channels, instead of the minimum as in DCP.

$$D(x) = \max_{x\in\Omega, c\in R} I^c(x) - \max_{x\in\Omega, c\in B,G} I^c(x),$$
$$\tilde{t}(x) = D(x) + (1 - \max_x D(x)). \quad (7)$$

Other variations of the DCP were proposed by Gibson *et al* [7]. They replace the second minimum in the Eq. 6 by the median operator, called MDCP. The median operator was chosen due to its ability to preserve edges. It avoids the refinement in the transmission, as proposed by He *et al.* [9, 11]. The MDCP is constructed as described by Eq. 8.

$$t(x) = 1 - med_{y\in\Omega(x)}(\min_{c\in R,G,B} \frac{I^c(y)}{A^c}). \quad (8)$$

2.4. UDCP Methodology

The statistic correlation of a low Dark Channel in haze-free images is not easy to be tested underwater due the difficulty to obtain real underwater images in an out of water condition. But, the assumptions made by He *et al.* [9, 11] are still plausible, *i.e* at least one color channel has some pixels whose intensity are close to zero. This low intensities are due to: a) shadows; b) objects or surfaces where at least one color is low intensity, *e.g* fishes, algae or corals; c) dark objects or surfaces, *e.g.* rocks or dark sediment.

Although, the dark channel assumption sounds acceptable, some problems with the wavelength independence is clearly false in most of the cases. In Fig. 1, we show two real underwater images where the DCP fails due to the red channel. The first column shows a typical situation where the red channel is nearly dark, thus it corrupted the transmission estimate by the standard DCP. Finally, we show an example in the last column where the red channel is approximately independent from the scene depth. It is important to observe the red channel representation, where small values and larger values are due to darker and lighter colors, respectively, hence, it is the opposite of the transmission, see Eq. 6.

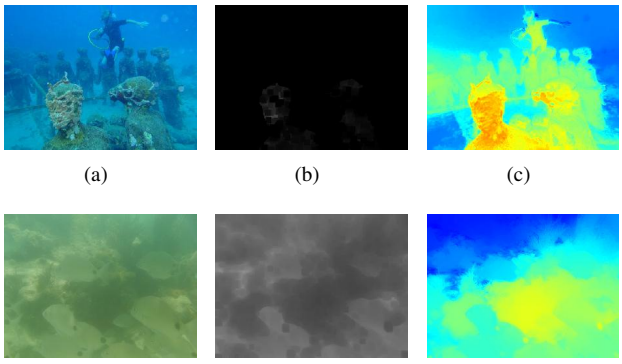

(a) (b) (c) (d) (e) (f)

Figure 1. Common situation where the red channel does not respect the wavelength independence and the relation with the depth. Two different underwater images[1] are shown in the first column. In the second column, it is shown the minimum of the red channel ($\min_{y\in\Omega} I^R(y)$). Last column show the colorized transmission estimated using UDCP.

Considering the aforementioned limitations in underwater conditions, we propose here a new version of DCP, which we call Underwater DCP (UDCP). In this case, the DCP is only applied in the green and blue channels. It is due the difficult to modeling the behavior of the red channel. This phenomena is mainly related to the high absorption effect in the red channel that imposes it to be near zero in a lot of situation.

Similarly to Eq. 5, Eq. 9 shows the UDCP proposed here.

$$J^{UDCP}(x) = \min_{y\in\Omega(x)} (\min_{c\in G,B} J^c(y)). \quad (9)$$

The airlight constant A is estimated by finding the brightest pixel in the underwater dark channel. Considering Eqs. 4 and 9, we isolate the transmission in a local patch $\tilde{t}$ as in the standard DCP. Applying the minimum operation to both sides, we can estimate $\tilde{t}$ based on the image I and the airlight A. Eq. 10 shows the estimation of $\tilde{t}$. As proposed by He *et al.* [9], we also use the spectral matting method to refine the estimated transmission. We defined the $\Omega(x) = 15 \times 15$.

$$\tilde{t}(x) = 1 - \min_{y\in\Omega(x)} (\min_{c\in G,B} \frac{I^c(y)}{A^c}). \quad (10)$$

[1]The credits of the images: 2.1) www.underwatersculpture.com; 2.2) [1].

3. Experimental Results

In this section, we evaluate three different image restoration methods in underwater conditions, all of them based on DCP. The standard DCP was applied in underwater images, as proposed by [3] [4]. The MDCP [7] was also applied to underwater images, but using refinement method as proposed by He *et al.* [9]. To the best of our knowledge, ours is the first work to demonstrate the method's performance in this type of environment. We also evaluate the Bianco's prior (BP) [2].

Fig. 2 shows the results obtained by applying the methods to images that we have captured as well as images acquired by other authors. Our images were acquired in the Brazil's Southeast Coast, approximately 17 nmi from the coast at a depth of 20 m using the underwater vehicle Seabotix LBV300-5 equipped with two colored cameras. For these images, the airlight was well balanced in all wavelengths due the characteristics of the water and the small water depth, *i.e.* the red channel suffers small absorption rate; some images were acquired with overlayed on-screen information (OSD) as the one in Fig. 2(u); the images contain part of the vehicle structure in the top left corner; and resolution of the captured images is 640×480.

In the first column of Fig. 2, we show the original images with the airlight A estimation. The yellow pixels are the 0.1% brightest pixels in the dark channel, as proposed by He *et al.* [9]. The red circle is the largest intensity pixel among these pixels. The orange circle is the estimation using the UDCP, where He's method is applied only to the G-B channels. Finally, the purple circle is the estimation based on the BP, where the farthest point from the camera is chosen.

The airlight estimation requires a completely haze-opaque region in the image, which usually occurs in a region above the horizon. The method proposed by He *et al.* [9] clearly fails in the estimation as shown in Fig. 2(f). In this case the airlight is detected on a rock. Using the UDCP, the airlight is correctly detected in every cases. Lastly, the estimation based on BP fails to find the airlight in the 2(a) and 2(k).

In Fig. 2, the refined transmission t is shown in the other columns. The results are colored in order to improve the visualization, where hot colors, *i.e.* reddish colors, represent closer points and cold colors, *i.e.* bluish colors, represent distant points.

It is easy to see that the standard DCP fails in the transmission estimation in some cases. This can be mainly seen in figs. 2(b) and 2(l). This is due to the low intensity of the red channel. Thus, the standard DCP is mostly composed by red channel information. Hence, both works [3, 4] that uses standard DCP can fail in this typical situation. In Fig. 2(g), the transmission seems overestimated, due the bad estimation of the airlight. The standard DCP and the UDCP attained the best results for the images we have acquired, *i.e.* the last two rows.

The UDCP and the MDCP results are presented in third and fourth columns in Fig. 2. They are similar and very impressive; as it can be seen in figs. 2(c) and 2(d). It is possible to see that the methods correctly identify the distance from the camera to the divers and rocks. Moreover, figs. 2(m) and 2(n) are also similar. The similarities occur due the low intensities of the red channel and the similar intensities in the green and blue channel, thus the median and the minimum of the blue and green channels present similar value. The largest difference between UDCP and MDCP, shown in figs. 2(h) and 2(i), is due to the red channel intensities. In the last two rows, there is a very small difference in the low intensity values of the transmission, where the UDCP is more plausible than the MDCP.

The last column in Fig. 2 shows the results obtained by BP. In figs. 2(e) and 2(o), it is possible to see the transmission are well estimated.Fig. 2(j) shows the results of BP, where the segmentation of the scene is overestimated but made in a correct way, with exception of the fishes.The last results are the worst obtained by the BP, where the method fails to estimate the transmission coefficient (see figs. 2(y) and 2(t)).

Quantitative results were obtained using two images from the Middlebury Stereo Dataset - Rocks1 [18] with different illumination, where the disparity maps are available. The model defined in Eq. 4 was applied in both images in order to simulate the underwater effects. In this case, the attenuation coefficient η and the airlight A was defined as proposed in [14] and [19], respectively. It allows us to simulate an oceanic water under variable chlorophyll concentration, defined by a constant C [14]. The depth map was obtained using previous knowledge about stereo baseline and focal distance that was multiplied by a 1.5 factor in order to increase the global distance and depth variation. The scene are far from the camera ($\approx 4m; \approx 6.5m$). We define $C = [0.05; 1.0]$ in the simulation. The ground truth transmission was selected as the green channel transmission, due the small global root-mean-square error (RMSE). The RMSE was used as metrics to evaluate the quality of evaluated methods.

Fig. 3 shows the results using simulation. Figs. 3(a) and 3(d) show the images obtained from the dataset. Figs. 3(b) and 3(e) show the Dark Channel Prior using all color channel, where it is possible to see that the assumption of darkness in almost true for the first case, but invalid in the second case. Figs. 3(c) and 3(f) illustrated the simulated images using $C = 0.5$. Both graphics in figs. 3(g) and 3(h) show the quantitative results, where the results obtained using BP are discarded in order to improve the visualization. For this case, it obtains $RMSE \approx [0.7; 0.9]$ for both cases.

Fig. 3(g) shows the simulated results for a low illumi-

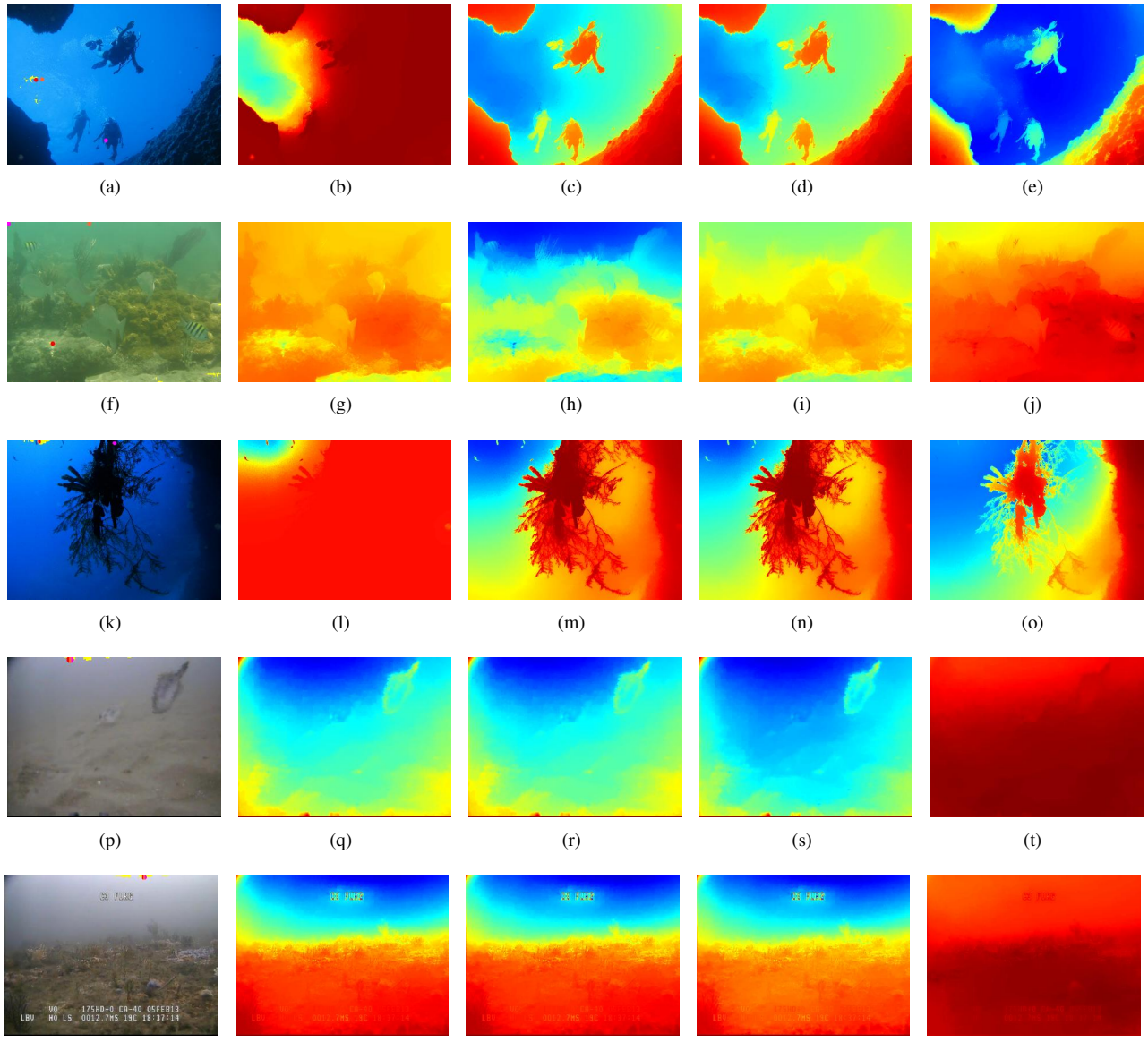

Figure 2. Evaluation the transmission estimation methods: First column - real underwater images[2] and airlight estimation, using DCP, in red, UDCP, in orange, and the BP, in purple; Colorized refined transmission t using standard DCP, in the second column, the UDCP, in the third column, the MDCP, in the forth column, and the BP, in the last column.

nation image, Fig.3(a). In this case, it is possible to see that the UDCP obtains the best results in almost all turbidity level. The largest error was obtained for smaller value of C. It is due the fact that little degradation images provides little information about the transmission. When the level of turbidity increases, the method is able to estimate the transmission until a limit where the information about the scene is lost. In this case, the transmission is almost null for the ground truth and estimation, thus the RMSE is small. Similarly, Fig. 3(h) shows the results for a high illumination image, Fig. 3(d). In this case the premises of the DCP fail, although all DCP based method are able to provide a good estimation. It is possible to see that the overall RMSE is larger than previous one. In this case, the MDCP obtains the best results with large turdibity level, and the UDCP overcoming the DCP. For smaller levels, the DCP and the UDCP obtain similar results with a some advantage to the UDCP.

[2]The credits of the images: 3(a) courtesy of Nick Roberts; 3(f) [1]; 3(k) freeunderwaterimages.com; 3(p),3(u) by the authors.

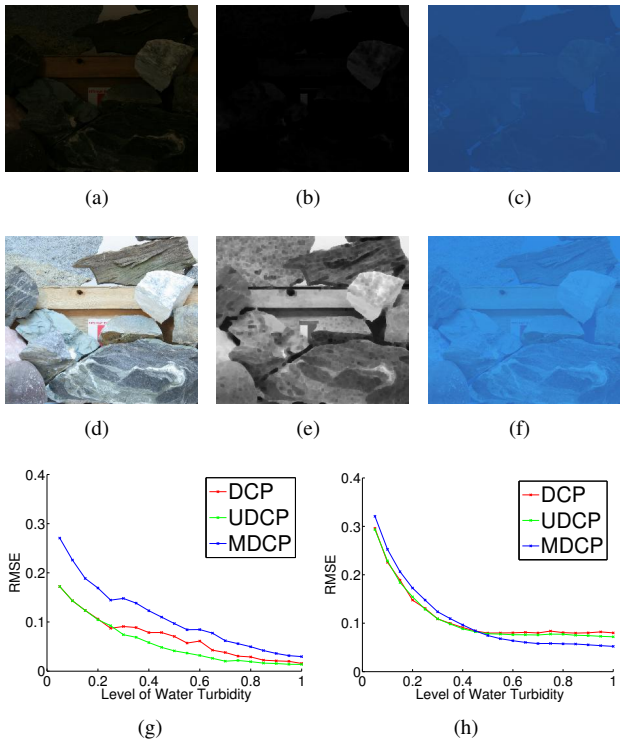

Figure 3. Quantitative evaluation the transmission estimation methods: First column - Images obtained from Middlebury Stereo Dataset; DCP of the original images, in the second column; Example of simulated underwater images using $C = 0.5$, in the third column; Quantitative results using RMSE, in the last row.

4. Conclusions and Future Directions

The DCP is a very intuitive and fast method. However it is limited in underwater conditions, due assumptions that are not always true. Other important limitation is related to the red channel. It suffers from high absorption rate, generating wrong estimations. The BP method presented good results in specific context. Typically, it underestimated the transmission. Furthermore, it needs to be further explored in terms of physical plausibility. The evaluated MDCP present more robustness in reduced intensity red channel. Finally, UDCP presents the most significant results in underwater conditions. It shows good results even in situations where other methods can fail.

Although the methods presented meaningful results, they lack both in the reliability and robustness. The use of single image methods to restore image can enhance the quality but is susceptible to the scene characteristics. Thus, the future directions seem to use video in order to disambiguate the parameters of the model. Acquiring video is a common capability in almost all model of underwater cameras used by divers and vehicles. In this case, the single image restoration methods can be a good initial estimation.

Acknowledgments

This research is partly supported of CNPq, CAPES, FAPEMIG and PRH-27 FURG-ANP/MCT. This paper is a contribution of the INCT-Mar COI funded by CNPq Grant Number 610012/2011-8.

References

[1] C. Ancuti, C. Ancuti, T. Haber, and P. Bekaert. Enhancing underwater images and videos by fusion. In *IEEE CVPR*, pages 81–88, 2012.

[2] N. Carlevaris-Bianco, A. Mohan, and R. Eustice. Initial results in underwater single image dehazing. In *IEEE OCEANS*, pages 1–8, 2010.

[3] L. Chao and M. Wang. Removal of water scattering. In *ICCET*, volume 2, pages 35–39, 2010.

[4] J. Chiang and Y. Chen. Underwater image enhancement by wavelength compensation and dehazing. *IEEE TIP*, 21(4):1756–1769, 2012.

[5] M. Ding and R. Tong. Efficient dark channel based image dehazing using quadtrees. *Science China Information Sciences*, pages 1–9, May 2012.

[6] R. Fattal. Single image dehazing. *ACM TOG*, 27(3), 2008.

[7] K. Gibson, D. Vo, and T. Nguyen. An investigation of dehazing effects on image and video coding. *IEEE TIP*, 21(2):662–673, 2012.

[8] D. He and G. Seet. Divergent-beam lidar imaging in turbid water. *Optics and Lasers in Engineering*, 41(1):217–231, 2004.

[9] K. He, J. Sun, and X. Tang. Single image haze removal using dark channel prior. In *IEEE CVPR*, pages 1956–1963, 2009.

[10] K. He, J. Sun, and X. Tang. Fast matting using large kernel matting laplacian matrices. In *IEEE CVPR*, pages 2165–2172, 2010.

[11] K. He, J. Sun, and X. Tang. Single image haze removal using dark channel prior. *IEEE TPAMI*, 33(12):2341–2353, 2011.

[12] J. Jaffe. Computer modeling and the design of optimal underwater imaging systems. *IEEE JOE*, 15(2):101–111, 1990.

[13] B. McGlamery. A computer model for underwater camera systems. In *SPIE 0208, Ocean Optics VI*, volume 208, pages 221–231, 1980.

[14] C. D. Mobley. *Light and Water: Radiative Transfer in Natural Waters*. Academic Press, 1994.

[15] S. Narasimhan and S. Nayar. Contrast restoration of weather degraded images. *IEEE TPAMI*, 25(6):713–724, 2003.

[16] E. Nascimento, M. Campos, and W. Barros. Stereo based structure recovery of underwater scenes from automatically restored images. In *SIBGRAPI*, pages 330–337, 2009.

[17] J. Queiroz-Neto, R. Carceroni, W. Barros, and M. Campos. Underwater stereo. In *SIBGRAPI*, pages 170–177, 2004.

[18] D. Scharstein and R. Szeliski. A taxonomy and evaluation of dense two-frame stereo correspondence algorithms. *IJCV*, 47(1/2/3):7–42, 2002.

[19] Y. Schechner and N. Karpel. Recovery of underwater visibility and structure by polarization analysis. *IEEE JOE*, 30(3):570–587, 2005.

[20] R. Tan. Visibility in bad weather from a single image. In *IEEE CVPR*, pages 1–8, 2008.